Focused magma supply at the intersection of the Cobb hotspot and Juan de Fuca ridge

(In review, February 2003)

Michael West[1], William Menke, and Maya Tolstoy

Lamont-Doherty Earth Observatory and Department of Earth and Environmental Science, Columbia University, Palisades, NY 10964

[1]Now at Department of Physics, New Mexico State University, Las Cruces, NM 88005

Abstract. We examine the interplay between the Cobb hotspot and the Juan de Fuca ridge by mapping the base of the crust near Axial Volcano. PmP traveltimes from an extensive active source seismic experiment are used in conjunction with prior crustal tomography to map crustal thickness. In addition to a previously-inferred increase in crustal thickness. A cross-section along the ridge axis consists of two distinct trends. In addition to 1-2 km of excess crust along a broad section of the central ridge, we find a 20-40 km diameter root extending to 11 km directly beneath the volcano. Focused magma flux from the Cobb hotspot (0.3-0.8 m^3/s) is inferred to be responsible for both the narrow root and the large magma reservoir at Axial. A transition back to ridge-dominated magmatism is observed away from the intersection.

1. Introduction

1.1. Hotspot-Ridge Interaction

There has been a growing consensus in recent years that mantle upwelling beneath ocean ridges is a passive response to the tectonic separation of the plates [Forsyth et al., 1998]. In contrast, hotspots supply magma from a buoyant plume or a warm/wet upper mantle heterogeneity with little regard for the state of the overlying crust. We use the term "hotspot" for any long-lived mantle magma source and reserve "mantle plume" for those hotspots which might have a deep mantle root (e.g. Hawaii [Zhang and Tanimoto, 1992] and Iceland [Shen et al., 1998]). Whether sourced from the upper or lower mantle, the persistence of intraplate hotspots argues strongly that they are not a response to plate motions. It is this independence that has allowed hotspots to become the reference frame against which most tectonic motions are measured.

Though large hotspots are known to interact with ridges as far as 1000 km away [Ma and Cochran, 1996; Schilling, 1991] each is the result of fundamentally different mechanisms. One is driven by plate motions; the other is largely independent. When they are co-located however the distinction between ridge and hotspot is no longer clear and one may question the singular existence of either. In this paper, we examine the interaction between the upper mantle Cobb hotspot and the medium spreading rate Juan de Fuca ridge.

Much of our understanding of hotspot-ridge interactions comes from the large hotspots of Iceland, Kerguelen, Galapagos, Amsterdam/St. Paul, Louisville and the Azores. Most of these systems have created substantial islands and platforms indicating large sustained magma fluxes with source diameters measured in hundreds of kms. These systems are so uniquely massive, however, that few similarities exist with the numerous small seamount chains that populate the oceans [Wessel and Lyons, 1997]. Given this, observations from mantle plume scenarios offer limited insight into the processes responsible for most of the thousands of seamounts on the ocean floors.

This study is motivated by a lack of understanding of the competing roles of ridge and hotspot magmatism, which stems largely from a poor characterization of small upper mantle hotspots. Characterizing how a ridge and hotspot perturb one another sheds light not only on their interaction, but more importantly on the mechanics of each system.

1.2. The Cobb hotspot / Juan de Fuca ridge system

An ideal place to explore this relationship is the superposition of the Cobb hotspot on the Juan de Fuca (JdF) ridge in the northeast Pacific (Figure 1). The Cobb-Eickelberg Seamount chain is age-progressive extending at least to 9 Ma [Desonie and Duncan, 1990], indicative of a hotspot source. Currently, the ridge and hotspot are colocated at Axial Volcano. The ridge segment which includes Axial is unlike any other on the JdF ridge. It has: 700 m of elevation above the rest of the ridge [Delaney et al., 1981]; a 50 mGal Bouguer gravity low [Hooft and Detrick, 1995]; a prominent caldera; evidence of centralized magma supply [Dziak and Fox, 1999; Fox, 1999]; a long-lived magma reservoir that is far larger than a typical eruption volume [West et al., 2001]; and rift zones which essentially constitute a segment of the JdF ridge.

Much of our understanding of the Cobb-JdF interaction at Axial comes from petrologic and gravity studies. Increased

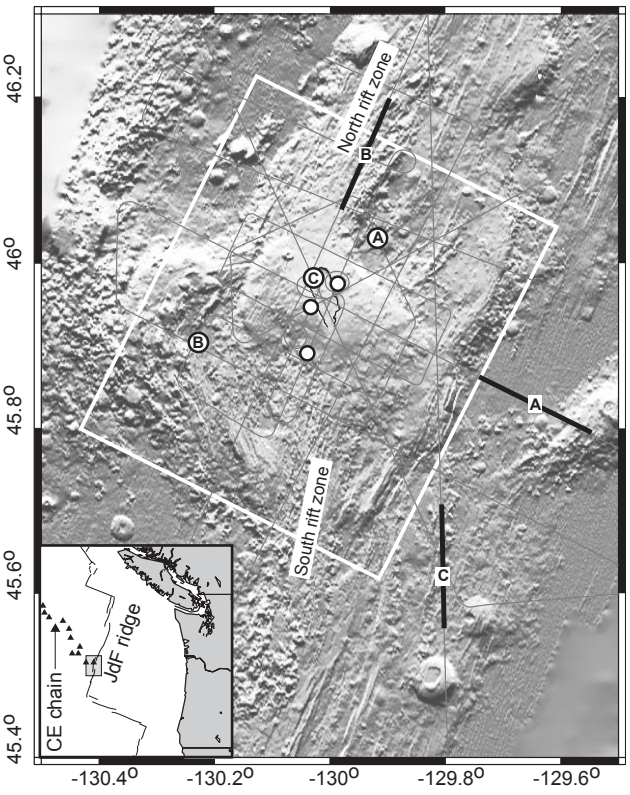

Figure 1. Map of the central JdF ridge and Cobb hotpot. The caldera floor of Axial Volcano (shaded) is 1450 m below sea level. The surrounding sea floor is ~2800 m. Airgun shots are marked with grey lines. White circles mark ocean bottom seismometers (OBS).

MgO content suggests melting beneath Axial begins deeper in the mantle and melts more than under the rest of the JdF ridge [Rhodes et al., 1990]. A gravity analysis estimates that the crust in the central portion of the JdF (centered on Axial) is 1.5-2 km thicker and mantle temperatures are elevated by 30-40° relative to the rest of the ridge [Hooft and Detrick, 1995]. These observations suggest a hot region of excess magma production in the upper mantle, as is expected from the coalescence of two separate melting features. We map the Moho near Axial to explore how passive upwelling beneath the ridge interacts with the localized melt supply of the Cobb hotspot.

2. Method

Axial Volcano was the target of an airgun-to-ocean bottom seismometer (OBS) experiment in April 1999. Several compressional wave arrivals are observed including the crustal turning wave Pg, Moho-reflected PmP and mantle-refracted Pn (Figure 2). The crustal velocity model of West et al. [2001] is dominated by a low velocity magma body 2.5-3.5 km below the caldera. At a depth of 6 km, compressional wave velocities of 7.0-7.2 km/s indicate the magma body does not extend into the deeper crust.

Early modeling of PmP phases suggested crustal thickness of ~8 km away from the caldera, which is in good agreement with gravity predictions. However, variations in PmP arrival times and Pg/Pn cross-over distance suggested significant relief on the Moho (Figure 2). 1677 PmP traveltimes, from 44 record sections, are picked using a waveform cross-correlation technique [West, 2001]. Since the traveltimes are a function of Moho depth and the overlying crustal structure, the prior tomography results are used to constrain the upper 6 km of crust. We address the inherent trade-off between lower crust velocity and Moho depth by assuming typical velocities and examining errors post priori. We append velocities to the bottom of the crustal model that increase linearly to 7.4 km/s on the topside of the Moho. Outside the resolved area, the crustal structure reverts to a regional 1-D model.

Preliminary PmP traveltimes are calculated via 3-D raytracing through a suite of models with Mohos at different depths. Raytracing is performed with the publicly-available Raytrace3d package [Menke, Submitted]. Each traveltime is bracketed by a shallow and deep raypath. We interpolate these to find the reflection point in three dimensional space which predicts zero traveltime error. Where multiple raypaths exist, we use the path of the first arriving PmP as it best corresponds to the picked traveltime. This set of reflection points is gridded with a smoothing constraint to obtain a Moho surface. Since the reflection point depends on the slope of the Moho, we iterate this procedure with updated models to accommodate the non-linearity of the problem. The solution converges in just three iterations, reducing the PmP traveltime misfit to 0.10 s., a reduction of 81% compared to a uniform 6 km crust. Error in the Moho depth is estimated at ±0.5 km (Table 1).

Table 1. Sources of error

Source	Error
Picking error[1]	0.02 s
through crustal model[2]	0.07 s
Error in lower crust velocity assumption[3]	0.06 s
PmP misfit in final model	0.10 s
Total PmP two-way traveltime error[4]	0.14 s
depth error of Moho:	0.5 km

[1]estimated error in the traveltime picks - 3 samples (0.02 s)
[2]Two-way traveltime error through upper/mid crust model
[3]For topside Moho Vp of 7.0-7.9 km/s (7.4 km/s in model)
[4]Summation assumes uncorrelated errors

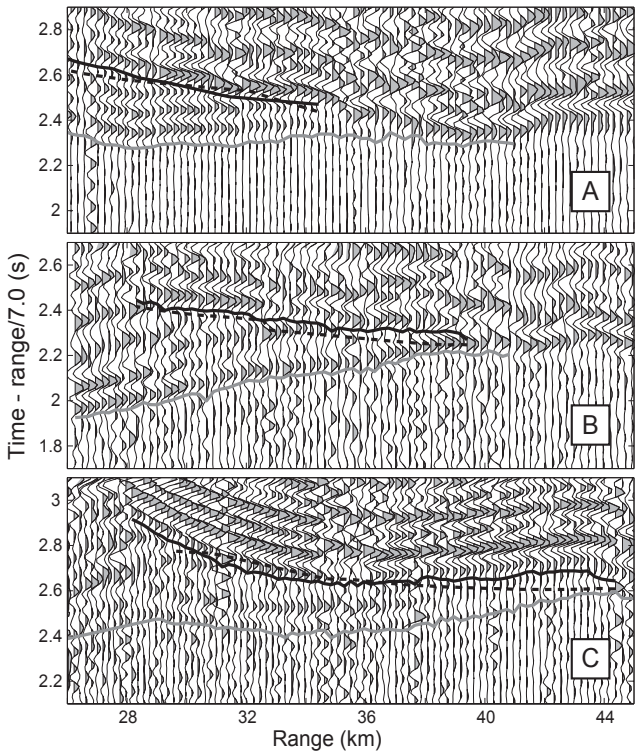

Figure 2. Waveforms for three geometries as labeled in Figure 1. Traces have been filtered (2-14 Hz) and adjusted for bathymetry. The crustal turning Pg phase is labeled in gray.

3. Observations

3.1. Moho topography

Crustal thickness is determined in a 50 km zone centered on the caldera (Figure 3). The crust thins away from Axial in both the ridge-parallel and ridge-perpendicular directions at the same rate, thinning from a maximum of 11 km beneath the caldera to 7-8.5 km at a distance of 15 km. The topography on the Moho mirrors that of the volcanic edifice — round and 20-40 km in diameter. The maximum crustal thickness is nearly twice that of typical oceanic crust. Variable crustal thickness has been observed on both fast and slow spreading ridges [e.g. Barth and Mutter, 1996; Hooft et al., 2000]. However, 11 km is much thicker than any unperturbed ridge segment — a clear response to the Cobb hotspot. Thickened crust has been observed at large oceanic hotspots including 15-17 km crust at the Marquesas [Caress et al., 1995] and 20 km crust beneath Hawaii [Watts et al., 1985]. These islands were formed far from ridges, with hotspot-derived material piled on top and underplated beneath pre-existing crust. Whereas at Axial, both hotspot- and ridge-derived magmas are emplaced more-or-less simultaneously.

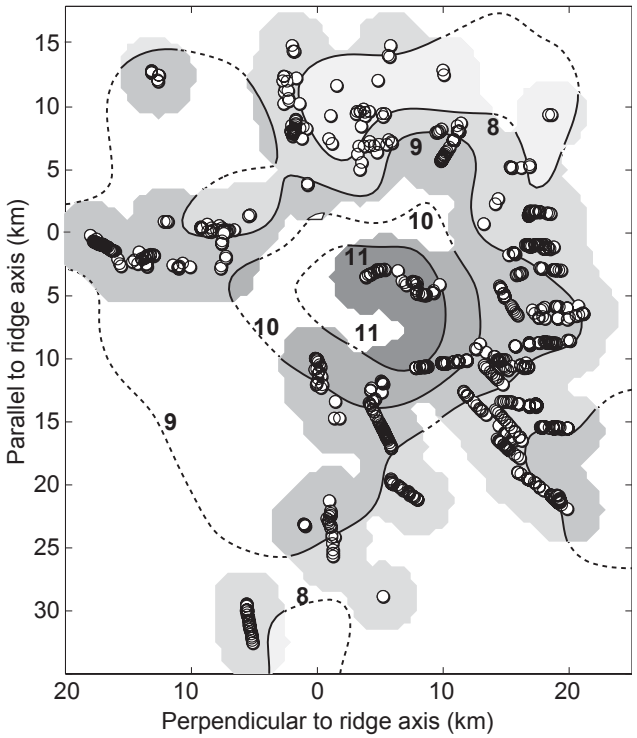

Figure 3. Map of crustal thickness. Area labeled as white box in Figure 1. PmP reflection points are labeled as circles. The crustal thickness of the final model is contoured in shades of gray. Unconstrained areas are masked out.

Thickened crust is common at hotspot-influenced ridges. The Iceland hotspot, on the Mid-Atlantic ridge, has produced crust in excess of 30 km [Darbyshire et al., 1998; Menke et al., 1998]. 2.3 km of thickening is observed along the Galapagos spreading center even though the hotspot is centered a few hundred km to the south [Canales et al., 2002]. These hotspots generate crust-forming partial melts at a rate greater than typical 6-7 km oceanic crust can accommodate. In response, the crust thickens along a broad section of the ridge, as has been inferred by gravity along the central JdF ridge. The root imaged in this study is a separate, much narrower feature in addition to the regional thickening.

3.2. Gravity

Because the root beneath Axial is narrow and deep, its gravitational signature is similar to a point mass centered 9-10 km below the sea surface. The signal decays rapidly at shallow depths and is below the noise level of the sea surface gravity measurements. Assuming a maximum plausible density contrast across the Moho of 400 kg/m^3, the peak signal in sea surface gravity would be 5 mGal. If the root is more dense and mafic than the overlying crust, as is observed in Iceland [Menke, 1999], the Marquesas [Caress et al., 1995] and Hawaii [Watts et al., 1985], its signature would be even smaller. Similarly, the root cannot explain the observed long wavelength 50 mGal Bouguer anomaly. The 100 km wide crustal thickening of 1-2 km found by Hooft and Detrick [1995] must be independent of the narrow root found here. If this gradual thinning is applied along the ridge outside the area of this study, the crust would reach a normal thickness of ~6 km near the ends of Axial's rift zones (Figure 4).

4. Discussion

4.1. Magma flux to Axial

Variations in Moho topography reflect differences in magma supply. A larger flux of melt creates thicker crust through underplating, dike emplacement and/or increased extrusion on the surface. Eleven km crust requires, at a minimum, 38-83% more melt than 6-8 km crust. If a narrow source beneath Axial is feeding the additional 1-2 km of crust along the rift zones as well (as is suggested by a down-rift dike eruption event [Dziak and Fox, 1999]), then the melt flux per km of ridge beneath Axial could exceed three times the normal flux of the JdF ridge, on par with fast spreading ridges. This high flux suggests that melting should be initiated at greater depths, as has been shown by higher Sr and lower silica saturation of Axial basalts [Rhodes et al., 1990].

If the Cobb hotspot is the source of the crustal thickening along the central JdF ridge (>6 km), and we use a full spreading rate of 5.5 cm/yr, the total magma flux from the Cobb hotspot is 0.3 m^3/s. If we assume the hotspot also provides half of the normal crust along the ridge segment comprised of Axial and its rift zones, the flux would be 0.8 m^3/s. This is 1/30th and 1/10th, respectively, of the estimated flux of the Iceland hotspot [Sleep, 1990].

The narrow root is strong evidence that Cobb magmatism is tightly focused under Axial, and that the melt supply is independent of the adjacent CoAxial and Vance segments of the ridge, as shown by Menke et al. [2002]. Though focusing toward segment centers is well known at slow spreading ridges, the mean crustal thickness remains several kms thinner than observed here. Limited Pn observations (not shown) support the notion of focused magmatism. Away from the caldera, apparent Pn velocities of 8.2 ± 0.4 km/s are higher than similar studies [e.g. Dunn et al., 2000; Menke et al., 1998] and inconsistent with widespread partial melt.

4.2 Magma transport

The influence of the Cobb hotspot on the central Juan de Fuca ridge is unmistakable. A 20-40 km wide melt supply corridor is inferred from Moho topography (Figure 4). The hotspot magma creates a local crustal root through underplating and the emplacement of sills and dikes. Some of the melt ascends to the mid-crustal magma body. This magma is distributed in the crust via surface eruptions and diking along the rift zones. The extra material emplaced along the segment-axis accounts for the 1-2 km of crustal thickening inferred from gravity. We propose that the long wavelength crustal thickening along the segment-axis is built from diking within the crust, while the local root beneath Axial is produced by augmentation of the lower crust.

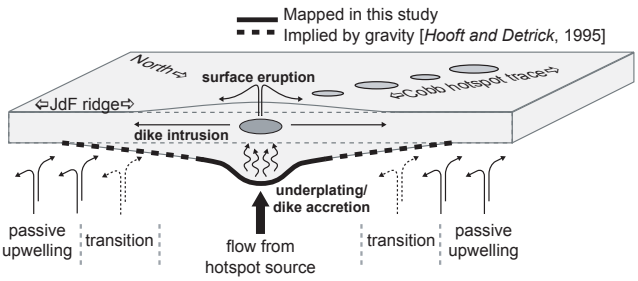

Figure 4. Schematic of magma supply at Axial.

4.3. Interaction between the ridge and hotspot

We propose two models to address the remaining question of how the hotspot source has impacted the background upwelling and melt supply associated with ridge spreading. We propose two models. In the first, the two melt supplies are additive. Hotspot melt migrates independent of, and superimposed on, the normal passive upwelling of the ridge. To first order, the total flux from the hotspot is equal to the production of excess crust along the central JdF ridge. In the second scenario, the flux of solid material from the hotspot is sufficient to accommodate the ridge spreading and thus shut down or decrease the upwelling of mantle beneath the ridge. In this model, the hotspot provides enough material to form much of the crust. Since the Cobb hotspot sources the same upper mantle as the JdF ridge, the composition of the crust would not differ significantly. However, the flow of the solid mantle matrix, which is not constrained by these data, would be quite different in each case.

Small seamounts along the segment erupt magmas that are less fractionated than basalts from the rifts, suggesting they are not fed from the central source [Perfit et al., 2001]. In addition, the range of K2O/TiO2 values along the rifts cannot be explained by fractionation alone, suggesting contributions from magma sources directly beneath the rifts. Interestingly, these seamounts and anomalous chemistries are mostly located toward the ends of the rift zones. This suggests a gradual transition from centralized hotspot magma supply to normal ridge mechanics away from Axial (Figure 4).

All evidence points to the Cobb hotspot playing a significant role in magma supply along the central Juan de Fuca ridge. Magma supply from the Cobb hotspot is tightly focused beneath Axial, and has built a thick narrow crustal root. In light of the large, previously-observed magma body, it is likely that a significant portion of the hotspot magma penetrates the crust and is redistributed via lateral dike injection and surface eruption. These magmas result in additional crust along a broad region of the ridge. Away from the volcano, the supply mechanism transitions back to locally-sourced magma produced by passive ridge upwelling.

Acknowledgments. We thank S. Webb, M. Perfit, J. Chadwick and M. Spiegelman for provocative discussions; R. Sohn for data preparation; and the crews of the RV Thomas G. Thompson and the RV Maurice Ewing who make marine science possible. This work was supported by the US National Science Foundation.

References

Barth, G.A., and J.C. Mutter, Variability in oceanic crustal thickness and structure; multichannel seismic reflection results from the northern East Pacific Rise, J. Geophys. Res., 101, 17,951-17,975, 1996.

Canales, J.P., G. Ito, R.S. Detrick, and J. Sinton, Crustal thickness along the western Galapagos spreading center and the compensation of the Galapagos hotspot swell, Earth Planet. Sci. Lett., 203, 311-327, 2002.

Caress, D.W., M.K. McNutt, R.S. Detrick, and J.C. Mutter, Seismic imaging of hotspot-related crustal underplating beneath the Marquesas Islands, Nature, 373, 600-603, 1995.

Darbyshire, F.A., I.T. Bjarnason, R.S. White, and O.G. Flovenz, Crustal structure above the Iceland mantle plume imaged by the ICEMELT refraction profile, Geophys. J. Int., 135, 1131-1149, 1998.

Delaney, J.R., H.P. Johnson, and J.L. Karsten, The Juan de Fuca Ridge-hot spot-propagating rift system; new tectonic, geochemical, and magnetic data, J. Geophys. Res., 86, 11,747-11,750, 1981.

Desonie, D.L., and R.A. Duncan, The Cobb-Eickelberg seamount chain; hotspot volcanism with mid-ocean ridge basalt affinity, J. Geophys. Res., 95, 12,697-12,711, 1990.

Dunn, R.A., D.R. Toomey, and S.C. Solomon, Three-dimensional seismic structure and physical properties of the crust and shallow mantle beneath the East Pacific Rise at 9 degrees 30'N, J. Geophys. Res., 105, 23,537-23,555, 2000.

Dziak, R.P., and C.G. Fox, The January 1998 Earthquake Swarm at Axial Volcano, Juan de Fuca Ridge: Hydroacoustic Evidence of Seafloor Volcanic Activity, Geophys. Res. Lett., 26, 3429-3432, 1999.

Forsyth, D.W., D.S. Scheirer, S.C. Webb, L.M. Dorman, J.A. Orcutt, A.J. Harding, D.K. Blackman, J. Phipps Morgan, R.S. Detrick, Y. Shen, C.J. Wolfe, J.P. Canales, D.R. Toomey, A.F. Sheehan, S.C. Solomon, W.S.D. Wilcock, and M.S. Team, Imaging the deep seismic structure beneath a mid-ocean ridge; the MELT experiment, Science, 280, 1215-1218, 1998.

Fox, C.G., In situ ground deformation measurements from the summit of Axial Volcano during the 1998 volcanic episode, Geophys. Res. Lett., 26, 3437-3440, 1999.

Hooft, E.E., and R.S. Detrick, Relationship between axial morphology, crustal thickness, and mantle temperature along the Juan de Fuca and Gorda Ridges, J. Geophys. Res., 100, 22499-22508, 1995.

Hooft, E.E.E., R.S. Detrick, D.R. Toomey, J.A. Collins, and J. Lin, Crustal thickness and structure along three contrasting spreading segments of the Mid-Atlantic Ridge, 33.5 degrees -35 degrees N, J. Geophys. Res., 105, 8205-8226, 2000.

Ma, Y., and J.R. Cochran, Transitions in axial morphology along the Southeast Indian Ridge, J. Geophys. Res., 101, 15,849-15,866, 1996.

Menke, W., Crustal isostasy indicates anomalous densities beneath Iceland, Geophys. Res. Lett., 26, 1215-1218, 1999.

Menke, W., studies of seismic tomography in a regional context, in Seismic Data Analysis and Imaging With Global and Local Arrays, edited by A. Levander, and G. Nolet, American Geophysical Union, Submitted.

Menke, W., M. West, B. Brandsdottir, and D. Sparks, Compressional and shear velocity structure of the lithosphere in Northern Iceland, Bull. Seis. Soc. Am., 88, 1561-1571, 1998.

Menke, W., M. West, and M. Tolstoy, Shallow-crustal magma chamber beneath the axial high of the CoAxial Segment of Juan de Fuca Ridge at the source site of the 1993 eruption, Geology, 30, 359-362, 2002.

Perfit, M.R., J. Chadwick, I. Ridley, R. Embley, I. Jonasson, P. Herzig, and M. West, Insights into Ridge-Hotspot Interaction on the Juan de Fuca Ridge: Geochemical investigation of Axial Seamount and adjacent rift zones, Abstract, EGS General Assemblies, 2001.

Rhodes, J.M., C. Morgan, and R.A. Liias, Geochemistry of Axial Seamount lavas; magmatic relationship between the Cobb hotspot and the Juan de Fuca Ridge, J. Geophys. Res., 95, 12,713-12,733, 1990.

Schilling, J.-G., Fluxes and excess temperatures of mantle plumes inferred from their interaction with migrating mid-ocean ridges, Nature, 352, 397-403, 1991.

Shen, Y., S.C. Solomon, I.T. Bjarnason, and C.J. Wolfe, Seismic evidence for a lower-mantle origin of the Iceland Plume, Nature, 395, 62-65, 1998.

Sleep, N.H., Hotspots and mantle plumes; some phenomenology, J. Geophys. Res., 95, 6715-6736, 1990.

Watts, A.B., U.S. Ten Brink, P. Buhl, and T.M. Brocher, A multichannel seismic study of lithospheric flexture across the Hawaiian-Emperor seamount chain, Nature, 315, 105-111, 1985.

Wessel, P., and S.N. Lyons, Distribution of large Pacific seamounts from Geosat/ERS 1; implications for the history of intraplate volcanism, J. Geophys. Res., 102, 22,459-22,475, 1997.

West, M., W. Menke, M. Tolstoy, S. Webb, and R. Sohn, Magma storage beneath Axial Volcano on the Juan de Fuca mid-ocean ridge, Nature, 413, 833-836, 2001.

West, M.E., The deep structure of Axial Volcano, Columbia University, New York, 2001.

Zhang, Y.-S., and T. Tanimoto, Ridges, hotspots and their interaction as observed in seismic velocity maps, Nature, 355, 45-49, 1992.